



A fluorous copper(II)–carboxylate complex which magnetically and reversibly responds to humidity in the solid state

Artur Motreff^a, Rosenildo Correa da Costa^a, Hassan Allouchi^b, Mathieu Duttine^c, Corine Mathonière^c, Carole Duboc^d, Jean-Marc Vincent^{a,*}

^a Université de Bordeaux, Institut des Sciences Moléculaires (CNRS-UMR 5255), Talence, France

^b Université de Tours, Laboratoire de Chimie Physique (PCMB-EA 4244), Tours, France

^c CNRS, Université de Bordeaux, ICMCB, 87 av. du Dr Schweitzer, 33608 Pessac, France

^d Université Joseph Fourier, Département de Chimie Moléculaire (CNRS-UMR 5250), Grenoble, France

ARTICLE INFO

Article history:

Received 7 January 2011

Received in revised form 4 March 2011

Accepted 7 March 2011

Available online 15 March 2011

Keywords:

Copper(II)–carboxylate complexes

Magnetic sponge

Fluorous chemistry

Coordination compounds

Humidity sensing

Solid state reactivity

ABSTRACT

Reacting the fluorous carboxylate $C_8F_{17}CO_2\cdot HNEt_3$ with $Cu(OTf)_2$ in acetone leads, depending on the carboxylate/copper ratio, either to the neutral dimeric complex $[Cu_2(C_8F_{17}CO_2)_4(\text{acetone})_2]$ (**2**), or to the dianionic monomeric complex $[Cu(C_8F_{17}CO_2)_4](HNEt_3)_2$ (**4**). Both complexes were characterized by IR, UV–vis and EPR spectroscopies, magnetic susceptibility measurements and X-ray diffraction analysis. The complex **2** displays the classical dimeric “paddlewheel” structure with four carboxylates bridging the two copper(II) ions while the complex **4** displays an unusual monomeric structure with four monodentate carboxylates bounded to the copper(II) in a square planar geometry. In contrast to **4**, the complex **2** shows a very high affinity for water vapors in the solid state and behaves as a magnetic sponge. When exposed to air, ground crystals of **2** rapidly trap up to 6 water molecules per copper ion leading to a decrease of the magnetic coupling from $2J = -480 \text{ cm}^{-1}$ to $2J = -7 \text{ cm}^{-1}$. The hydration process is accompanied by drastic changes of the EPR and FTIR spectra, revealing that the binding of the water molecules to the copper atoms leads to the release of the acetone ligands from the solid and to the shifting of two carboxylates from bridging bidentate to non-bridging monodentate coordination mode. When hydrated **2** is exposed to high vacuum, the water molecules are removed from the solid. The dehydration process leads to the partial recovery of the antiferromagnetic coupling between the copper(II) ions as revealed by EPR and magnetic susceptibility measurements. These data show that the hydration/dehydration process is not accompanied by a fully reversible structural rearrangement in the solid state. The unusual affinity for water and consequently, the modification of the magnetic properties, is observed neither with the fluorous dimeric complex **1**, nor with the dianionic monomeric complex **4**.

© 2011 Elsevier B.V. All rights reserved.

Our research within the group “Nanostructures Organiques” of the “Institut des Sciences Moléculaires” in Talence focuses on the area of fluorous chemistry. We are interested in developing new methodologies to reversibly transfer non-fluorinated compounds from hydrocarbon to perfluorocarbon phases, by exploiting coordination chemistry and supramolecular interactions. These methodologies can be applied to catalyst recycling, multi-step synthesis or the colorimetric detection/titration of analytes such as ethanol. Recently, we are getting interested in the area of surface modifications (SiO_2 , Teflon) based on adsorption processes of highly fluorophilic copper(II)–carboxylate complexes.

1. Introduction

Copper(II)–carboxylate complexes are among the most widely studied coordination compounds [1]. In most cases such complexes exhibit the chemical formula $[Cu_2(OOCR)_4L_2]$ with the typical neutral “paddlewheel” structure in which the four carboxylates bridge the two copper(II) ions in a syn-syn configuration affording two accessible coordination sites in apical positions for monodentate L ligands, typically a solvent molecule such as pyridine [2], THF [2], CH_3CN [2,3], DMA [2], acetone [3], $EtOH$ [3], or water [4,5]. Such complexes, with their well-defined rigid dimeric structure, have been the subject of intense studies, particularly related to their magnetic properties [6], their incorporation as building blocks in Metal-Organic-Frameworks (MOFs) [7], or their catalytic activity [8]. On a more fundamental point of view, their very rich coordination chemistry, due to the lability of the carboxylate ligands and the diversity of their coordination modes, has led to the preparation and characteriza-

* Corresponding author. Fax: +33 540006158.

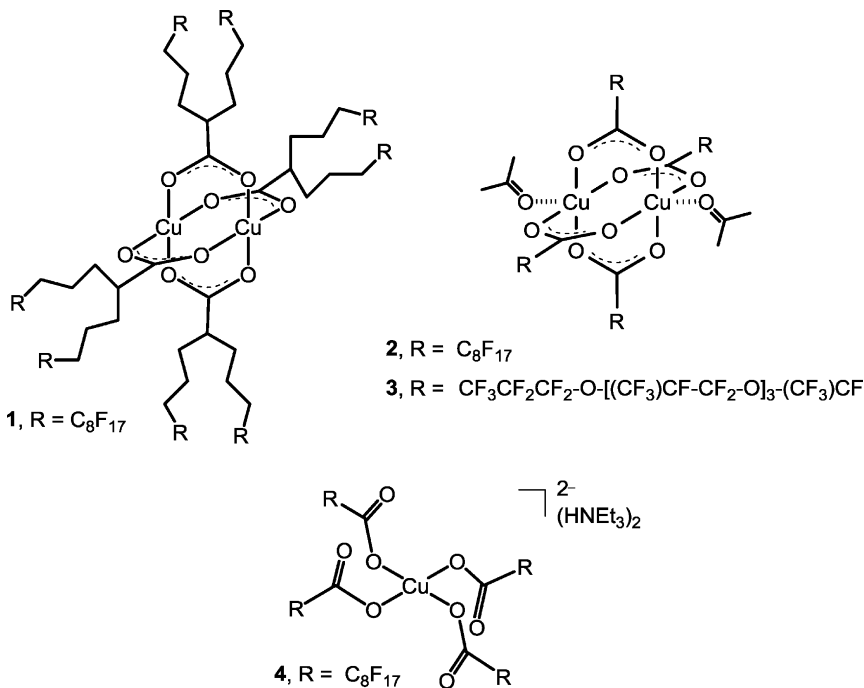
E-mail address: jm.vincent@ism.u-bordeaux1.fr (J.-M. Vincent).

tion of numerous copper(II)-carboxylate complexes exhibiting a variety of monomeric and dimeric structures [9]. The solution coordination chemistry of the dimeric “paddlewheel” copper(II) carboxylates has been extensively investigated. In particular, it has been shown that electron-poor carboxylates (such as trifluoroacetate anion and α -halogenated carboxylates) tend to favor monomeric copper(II)-carboxylate structures due to weaker Cu–O_{carb} bonds [1a–c].

Since 2002, we have investigated the coordination chemistry of fluorous copper(II)-carboxylate complexes **1–3** for various applications [10]. For instance, the highly fluorophilic complex **1** has been used to reversibly transfer pyridyl-tagged compounds such as porphyrins from a hydrocarbon to a perfluorocarbon phase [11]. The switching procedure was successfully applied to catalyst recycling [12], the purification of organic products in a multistep synthesis [13] or the development of a colorimetric assay for the visual detection and titration of EtOH in hydroalcoholic solutions and gasoline [14].

to the removal of the acetone ligands and the partial shifting of the carboxylates from a syn-syn bridging to a monodentate coordination mode (Scheme 1). Such solid-state transformation is very efficient as it is complete in approximately 4 h.

The study of solid materials exhibiting guest-modulated spectroscopic or magnetic properties is of great interest in light of potential application in sensing. As far as water detection is concerned, the materials described so far are mostly based on porous or nanoporous purely inorganic or mixed inorganic/organic coordination polymers with long-range ordering [18]. The term “magnetic sponge” has been introduced by Kahn [19] to define materials for which the magnetic properties are reversibly modulated upon the adsorption/desorption of water. We wish to report here that the complex **2** in the crystalline state behaves as a “magnetic sponge”. The removal of the water molecules in hydrated **2** leads to the partial recovery of the magnetic properties of **2** as shown by magnetic susceptibility and EPR measurements.



More recently, we have developed straightforward surface modification methodologies based on the unique physico-chemical properties of the dimeric complexes [Cu₂(C₈F₁₇CO₂)₄(acetone)₂] (**2**) and [Cu₂(C₁₄F₂₉O₄CO₂)₄(acetone)₂] (**3**) with fluorous electron deficient carboxylates. We showed that **2** and **3** can be very efficiently adsorbed on SiO₂ [15] and Teflon [16] surfaces leading to a strong and homogeneous covering by these complexes. Such surfaces can then be easily post-modified by molecules, such as pyridyl-tagged porphyrins, which can bind to the accessible coordination sites of the copper(II)-carboxylates. Interestingly, while being fluorophilic, the copper ions in complexes **2** and **3** exhibit a very high affinity for water. For instance, we showed that when ground crystals of **2** are exposed to air, up to six water molecules per copper ion are rapidly absorbed by the solid [17]. The water absorption is accompanied by a drastic change of the magnetic properties of the solid coupled to a dramatic change of its EPR spectrum [17]. Such behavior was explained by profound structural rearrangements occurring in the solid state upon binding of the water molecules to the copper ions, which leads

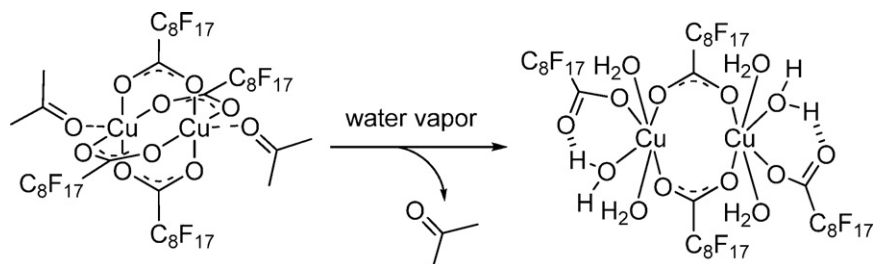
2. Results and discussion

2.1. Synthesis and structural characterization of complexes **2** and **4**

The dimeric complex **2** was prepared by reacting 2 equiv. of the triethylammonium salt of the perfluorinated carboxylic acid with Cu(OTf)₂ in acetone [17]. Large blue green parallelepipedic crystals of **2** were grown by allowing the solution to stand at 4 °C for several days. Using the same procedure but increasing the stoichiometry of the carboxylate to 4 equiv. leads to a deep blue acetone solution which affords selectively large parallelepipedic deep blue crystals of **4**. In some synthesis of **2**, both crystals can be obtained in the same reaction batch.

Single crystal analyses were performed on **2** and **4** affording the structures presented in Figs. 1 and 2, respectively.

Complex **2** displays the classical paddlewheel structure with four carboxylates in a syn-syn configuration bridging the two copper ions, while the acetone molecules occupy axial coordination sites leading to a square pyramidal coordination for each Cu



Scheme 1. Proposed structural rearrangement occurring in the solid state upon hydration of **2** under air.

atom (Fig. 1 and Table 2). The Cu–Cu distance (2.7375(8) Å) and Cu–O (basal) average distance (1.9735[13] Å) are close to those observed for the related dimer with trifluoroacetate ligands $[\text{Cu}_2(\text{CF}_3\text{CO}_2)_4(\text{CH}_3\text{CN})_2]$ (Cu–Cu = 2.766(1) Å, Cu–O (basal) = 1.969[5] Å) [20]. Consistent with the increase of the Cu–O (carb.) bond ionicity the Cu–Cu distance is significantly increased compared to that in $[\text{Cu}_2(\text{CH}_3\text{CO}_2)_4(\text{H}_2\text{O})_2]$ (Cu–Cu = 2.616(1) Å) [21]. The Cu–O distance for the apical acetone ligands (2.135(4) Å) is close to that found for the apical water ligands in $[\text{Cu}_2(\text{CH}_2\text{FCO}_2)_4(\text{H}_2\text{O})_2]$ (2.131(4) Å) [22]. For two of the four perfluorooctyl chains, the $\text{C}_\gamma\text{–C}_\delta$ bond adopts a gauche conformation, while all the other C–C bonds display the anti geometry. Such isomerization is most probably induced by crystal

packing effects and leads to both intra- and intermolecular interactions between the fluoroalkyl chains (Fig. 1 and Table 1).

The copper complex $[\text{Cu}(\text{C}_8\text{F}_{17}\text{CO}_2)_4](\text{HNEt}_3)_2$ (**4**) displays a unique structure with four monodentate carboxylate ligands lying in the same plane than the copper atom affording a square-planar geometry and a dianionic complex with triethylammonium as counter-cations (Fig. 2). To the best of our knowledge there are only a few examples of copper–tetracarboxylates with a square planar geometry. For instance, in the X-ray structure of $[\text{Na}_2\text{Cu}(\text{CH}_3\text{COO})_4(\text{H}_2\text{O})]\text{H}_2\text{O}$ reported by Spiccia and coworkers the sodium ions bridge square planar $[\text{Cu}(\text{CH}_3\text{COO})_4]^{2-}$ to form 2D sheets of $\text{Na}_2\text{Cu}(\text{CH}_3\text{COO})_4$ [23]. In this structure the acetates are coordinated to both copper and sodium ions, and arranged such as

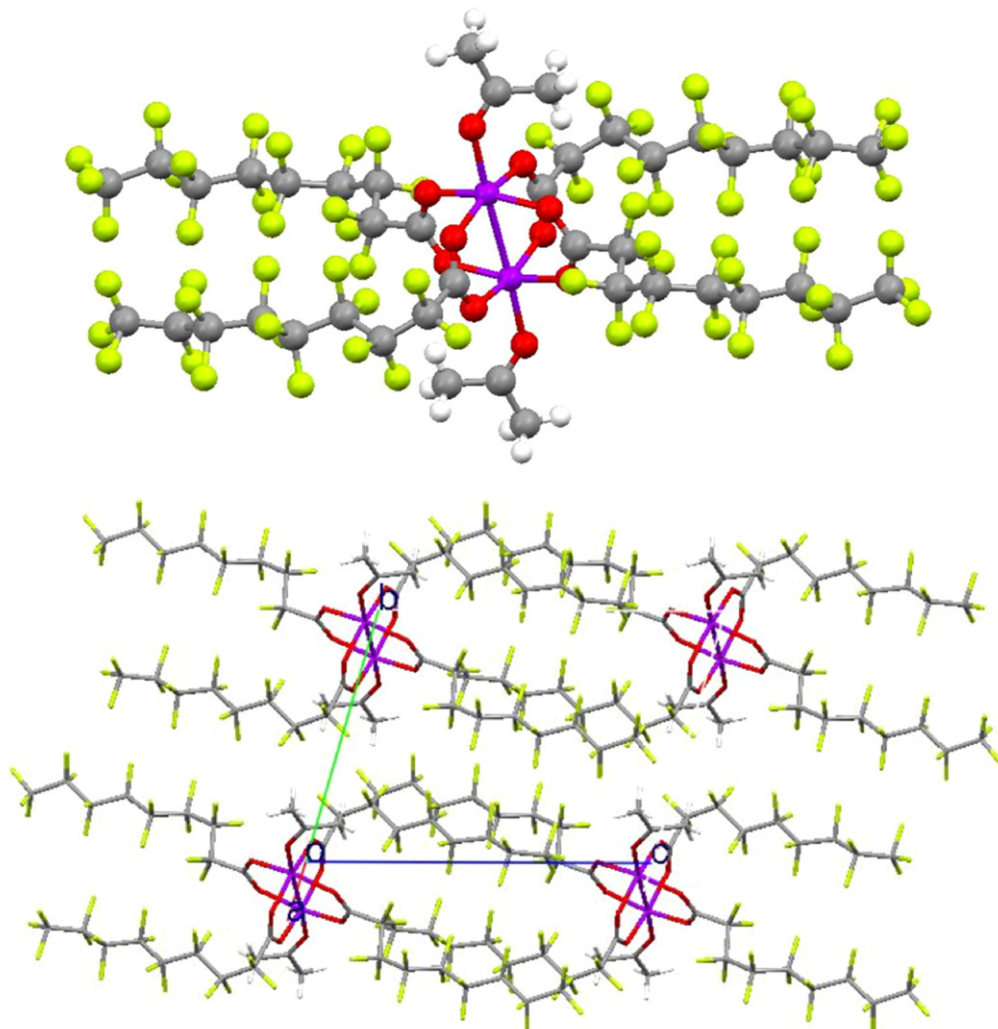


Fig. 1. Molecular structure of $[\text{Cu}_2(\text{C}_8\text{F}_{17}\text{CO}_2)_4(\text{acetone})_2]$ (**2**) and view of the crystal packing.

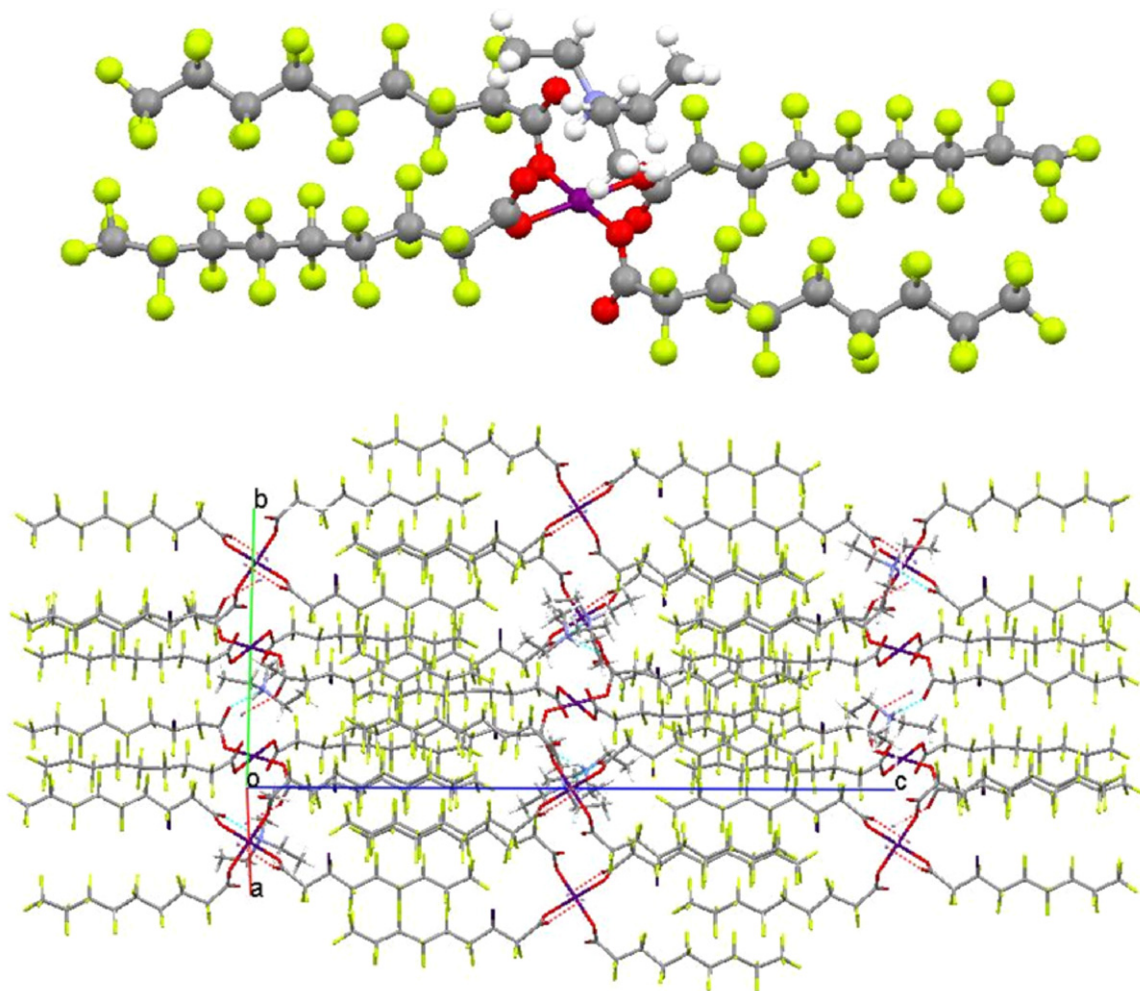


Fig. 2. Molecular structure of $[\text{Cu}(\text{C}_8\text{F}_{17}\text{CO}_2)_4](\text{HNEt}_3)_2$ (**4**) and view of the crystal packing.

Table 1
Summary of crystal data of **2** and **4**.

	2	4
Chemical formula	$\text{C}_{42}\text{H}_{12}\text{Cu}_2\text{F}_{68}\text{O}_{10}$	$\text{C}_{48}\text{H}_{32}\text{CuF}_{68}\text{N}_2\text{O}_8$
Formula weight	2095.52	2119.05
Temperature (K)	125(2)	150(2)
Wavelength (Å)	0.71073	0.71073
Crystal system	Triclinic	Orthorhombic
Space group	P-1	Pbca
<i>a</i> (Å)	9.92520(10)	10.3234(15)
<i>b</i> (Å)	11.9339(2)	19.225(3)
<i>c</i> (Å)	14.6689(2)	36.002(4)
α (deg)	71.0870(10)	90
β (deg)	83.3690(10)	90
γ (deg)	81.2620(10)	90
Volume (Å ³)	1620.52	7145.22
<i>Z</i>	2	8
Density (g cm ⁻³)	2.147	1.971
Absorption coefficient (mm ⁻¹)	0.906	0.535
<i>F</i> (000)	1014	4156
Crystal size (mm)	0.43 × 0.29 × 0.12	0.15 × 0.12 × 0.05
$2\theta_{\max}$ (deg)	31.61	27.06
Observed reflections	9769	8003
Variable reflections	6870	4459
Refinement method	Full-matrix least-squares on F^2	
Goodness-of-fit on F^2	1.089	1.142
Final <i>R</i> indices	$R_1 = 0.073$, $wR_2 = 0.227$	$R_1 = 0.0781$, $wR_2 = 0.1507$

adjacent acetates lie on opposite sides of the plane defined by the copper coordination plane. Two $[\text{Cu}(\text{betaine})_4]^{2+}$ complexes are also found; they adopt a square-planar geometry with similar up/down/up/down conformation for the ligands [24]. In the case of **4**, discrete mononuclear complexes are observed with the adjacent carboxylates lying in the same side of the plane defined by the copper coordination plane affording an up/up/down/down conformation. This conformation is most probably favored to minimize steric interaction with the bulky triethylammonium cations which tightly interact with the anion on each side of the copper coordination plane through a short hydrogen bond between the N-H and one C=O ($\text{H} \cdots \text{O} = 1.90 \text{ \AA}$). The Cu atom shows almost idealized square-planar coordination ($\text{O}-\text{Cu}-\text{O}_{\text{cis}} = 88.2(3)$ and $91.8(3)$, $\text{O}-\text{Cu}-\text{O}_{\text{trans}} = 180(3)$) with an average C–O distance ($1.929[6] \text{ \AA}$) slightly

Table 2
Selected bond lengths (Å) for some copper carboxylates.

Compound	$\text{Cu}-\text{O}_{\text{av}}$ (basal)	$\text{Cu}-\text{O}$ or $\text{Cu}-\text{N}$ (apical)	$\text{Cu} \cdots \text{Cu}$
$[\text{Cu}_2(\text{C}_8\text{F}_{17}\text{CO}_2)_4(\text{acetone})_2]$	1.9735[13] ^a	2.135(4)	2.7375(8)
$[\text{Cu}_2(\text{CF}_3\text{CO}_2)_4(\text{CH}_3\text{CN})_2]$	1.969[5]	2.114(2)	2.766(1)
$[\text{Cu}_2(\text{CH}_3\text{CO}_2)_4(\text{H}_2\text{O})_2]$	1.969[25]	2.156(4)	2.616(1)
$[\text{Cu}_2(\text{CH}_2\text{FCO}_2)_4(\text{H}_2\text{O})_2]$	1.969[17]	2.131(4)	2.674(1)
$[\text{Cu}(\text{C}_8\text{F}_{17}\text{CO}_2)_4](\text{HNEt}_3)_2$	1.929[6]		
$\text{Na}_2\text{Cu}(\text{CH}_3\text{COO})_4$	1.960[27]		
$[\text{Cu}(\text{betaine})_4]^{2+}$	1.948[0]		

^a The maximal deviation from the average is given in square brackets.

shorter than those found in $\text{Na}_2\text{Cu}(\text{CH}_3\text{COO})_4$ (1.960[27] Å) and $[\text{Cu}(\text{betaine})_4]^{2+}$ (1.948[0] Å). Differently from **2**, all the C–C bonds of the perfluoroalkyl chains display the anti geometry. For both **2** and **4**, the crystal packing view reveals two clearly separated domains due to a phase segregation between the apolar perfluoroalkyl chains and the polar copper(II)–carboxylate domains.

The attenuated total reflectance–Fourier transform infrared (ATR-FTIR) spectrum of **4** recorded on crystals exhibits two asymmetric C=O stretching vibrations at 1700 and 1670 cm^{–1}, the latter being less intense and attributed to the C=O interacting with the N–H through a hydrogen bond. The symmetric C=O stretching vibration of the monodentate carboxylates is observed at 1366 cm^{–1}. For comparison the asymmetric and symmetric vibrations are, respectively, found at 1678 and 1434 cm^{–1} for the bridging carboxylates of **2**, while the acetone C=O vibration is found at 1714 cm^{–1} (see the spectrum a in Fig. 4).

The temperature dependence of the $\chi_M T$ for **4** measured from 300 to 2 K under a field strength of 1 T is in agreement with a $S = 1/2$ mononuclear compound as the $\chi_M T$ value of 0.44 cm³ mol/K is constant with the temperature. This experimental value gave us a Zeeman factor $g = 2.17$. The powder X-band EPR spectrum of **4** at 100 K exhibits a rhombic $S = 1/2$ signal with $g_x = 2.312$, $g_y = 2.078$ and $g_z = 2.019$. Hyperfine coupling to Cu is only resolved on the g_x component with $A_x = 159$ G. These data are consistent with mononuclear Cu(II) complex with a $d_{x_2-y_2}$ ground state.

2.2. Hydration/dehydration process of **2** in the solid state: influence on the magnetic and spectroscopic properties

Recently, we reported that **2** in the solid state (ground crystals) when exposed to air can rapidly trap up to six water molecules per copper ion in a few hours. This process leads to a profound rearrangement of the coordination copper atoms such as a carboxylate shift from bridging bidentate to non-bridging monodentate coordination mode as illustrated in Scheme 1 [17]. Such solid-state structural rearrangement has been conveniently followed by ATR-FTIR spectroscopy (see the spectra a and b in Fig. 4) showing that, upon hydration, the acetone ligands are released from the solid, while a new C=O band at 1623 cm^{–1} appears, attributed to the monodentate carboxylates interacting with coordinated water molecule through an intramolecular hydrogen bond (Scheme 1). The moisture sensitivity of copper(II)–carboxylates derived from halogenated carboxylic acids has already been noticed. In solution, they generally adopt a mononuclear structure in the presence of coordinating solvents, apparently due to the weakening of the Cu–Cu interaction. Notably, neither the dianionic complex **4** with its particular square-planar geometry with four perfluor-

o carboxylates, nor the dicopper complex **1** in which the electron-withdrawing effect of the perfluoroalkyl chains is strongly reduced due to the alkyl spacer, shows affinity for water as checked by IR spectroscopy.

Of particular interest was the observation that the hydration of **2** led to a very fast and drastic change of the powder EPR spectrum (Fig. 3). When exposed to air (relative humidity = 60%), the excited state $S = 1$ spectrum of **2** ($g_{x,y} = 2.057$, $g_z = 2.372$, $D = 0.405$ cm^{–1}, $E/D = 0$) observed at room temperature rapidly disappears with the concomitant development of an intense rhombic spectrum typical of an $S = 1/2$ species ($g_x = 2.41$, $g_y = 2.096$, $g_z = 2.052$) attributed to magnetically isolated copper(II) ions of hydrated **2**. The transformation is fast, with about 65% of the solid transformed within 5 min, and highly efficient as the signal of **2** completely disappears within 4 h. Such changes in the EPR spectra upon hydration are the result of a drastic modification of the magnetic exchange interaction between the two copper(II) ions, as revealed by the magnetic susceptibility measurements (Fig. 6).

Magnetic measurements performed on the hydrated powder of **2** confirm the quantitative transformation of **2** in which the copper ions are strongly antiferromagnetically coupled ($2J = -480$ cm^{–1}, $g = 2.3$) into a structure in which the copper(II) ions behave as magnetically isolated ions at room temperature, but with still a small antiferromagnetic coupling between the metal ions ($2J = -7$ cm^{–1}, $g = 2.2$). Overall, the IR, EPR and magnetic data allowed us to propose for hydrated **2** the chemical structure presented in Scheme 1. Additionally, hydrated **2** exhibits similar spectroscopic (IR, EPR) and magnetic properties to the structurally characterized copper(II)–carboxylate dimer $[\text{Cu}_2(\text{C}_6\text{H}_3\text{Cl}_2\text{OCH}_2\text{COO})_4(\text{bipyam})_2]$ possessing two bridging and two monodentate carboxylates [25].

To study the eventual reversibility of the process, we have performed the dehydration of hydrated **2** under vacuum and the transformation was followed by ATR-FTIR. After standing for 4 h at 7×10^{-5} mbar, the removal of the water molecules from the solid is observed as revealed by the disappearance of the characteristic O–H stretching vibrations between 3700 and 3000 cm^{–1} (Fig. 4, spectrum c). At the same time, the coalescence of the two asymmetric C=O stretching vibrations was observed affording a single band at 1662 cm^{–1}, a value close to that found in **2** (1678 cm^{–1}). Upon dehydration the symmetric C=O stretching vibration is significantly shifted to higher frequency (from 1424 cm^{–1} to 1437 cm^{–1}) to reach the value found in **2** (1435 cm^{–1}). These changes would suggest that after dehydration the carboxylates present a coordination mode similar to that in **2**, that is bridging bidentate.

However, as discussed below, the EPR study is not consistent with the recovery of the “paddlewheel” structure found in **2**.

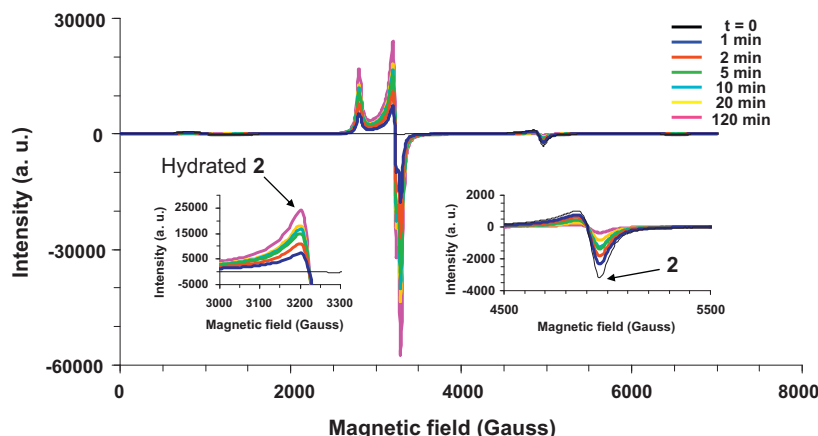


Fig. 3. Evolution of the room temperature X-band EPR spectrum of powdered **2** exposed to air.

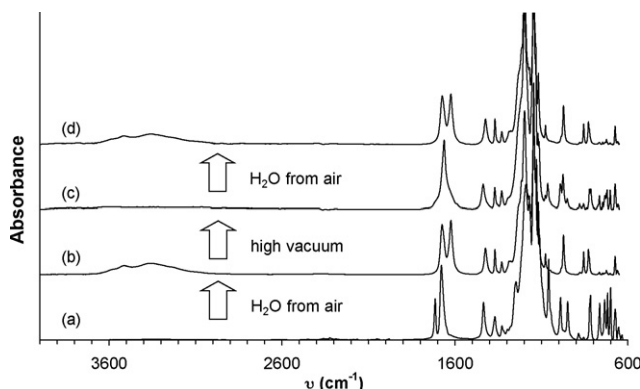


Fig. 4. ATR-FTIR spectra of solid samples of (a) **2**, (b) after exposure of powdered **2** in air for 45 min corresponding to fully hydrated **2**, (c) after exposure of hydrated **2** to high vacuum (7×10^{-5} mbar) for 4 h and, (d) after re-exposure of the same sample to air for \sim 15 min.

Exposing the dehydrated sample to air for \sim 15 min led to the full recovery of the IR spectrum of hydrated **2** implying that the structure proposed for hydrated **2** (Scheme 1) is certainly recovered during this process.

As shown in Fig. 5 the powder EPR spectrum of **2** is very sensitive to its hydration state. Dehydration of hydrated **2** is accompanied by an almost disappearance of its characteristic EPR spectrum which strongly suggests that antiferromagnetic coupling is, to some extent, recovered between the copper ions. Importantly, after dehydration (spectrum c) the characteristic signals corresponding to the initial paddlewheel structure of **2** (spectrum a) were never observed, showing that the structural transformation occurring in the solid state from **2** to hydrated **2** is not fully reversible when removing water. It has to be noted that, in any case, the structure of **2** with the two acetone ligands could never be recovered as the acetone is lost during the hydration process. Rehydration led to the fast recovery of the intense signal corresponding to magnetically isolated copper(II) ions (spectrum d). A reversible magnetic process thus occurs, which is directly correlated to the hydration/dehydration state of **2**.

Magnetic measurements confirm the partial recovery of the antiferromagnetic coupling between the copper(II) ions occurring during the dehydration process (Fig. 6). The $\chi_M T$ vs T curve of the dehydrated-hydrated **2** that continuously decreases from $0.6 \text{ cm}^3 \text{ mol/K}$ at 300 K to $0.2 \text{ cm}^3 \text{ mol/K}$ at 2 K is located between the $\chi_M T$ vs T curves of the original **2** and the dehydrated **2** suggesting a mixture of several forms of **2**. But all the attempts to satisfactorily fit the susceptibility data with the Bleaney–Bowers equation failed, even by considering a mixture of original **2** and

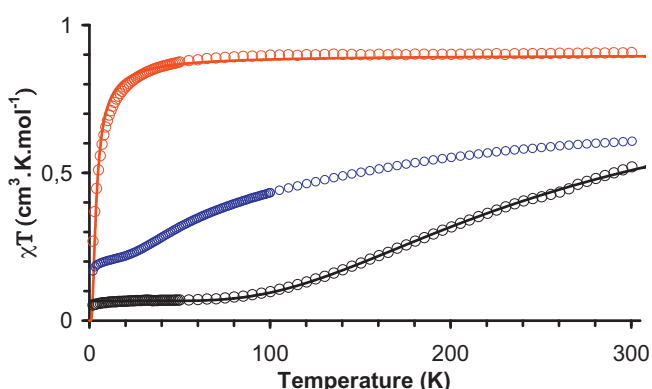


Fig. 6. Experimental (○) and calculated (—) magnetic susceptibilities plotted as χT vs T of crystals of **2** (black), hydrated **2** obtained from powdered crystals of **2** exposed to air for 24 h (red) and hydrated that have been dehydrated under vacuum (blue). (For interpretation of the references to color in this figure legend, the reader is referred to the web version of the article.)

hydrated **2**. It shows that after dehydration a mixture of species are obtained within the solid. When fully dehydrated, **2** could then be considered as an “unligated” copper(II)–carboxylates. Interestingly, Cotton et al. have shown that the “unligated” copper(II)–trifluoroacetate complex, in the crystalline state, forms an extended chain of dimers connected by carboxylates adopting a syn-anti geometry between two copper ions separated by 5.136 \AA [26]. In the case of **2**, after dehydration, the formation of such an extended chain the dimers bridged by carboxylates with a syn-anti geometry is unlikely as the shortest intermolecular $\text{Cu} \cdots \text{Cu}$ distance found in the crystal of **2** is too long (7.5 \AA) to allow such arrangement. We thus propose that after dehydration, the solid is still formed of discrete dimeric copper(II) complexes with bridging carboxylates.

3. Conclusion

The fluorous dimeric copper(II)–carboxylate complex **2** with the classical paddlewheel structure behaves as a magnetic sponge. In the solid state, its magnetic properties are markedly and reversibly modulated depending on its hydration state. The very fast and efficient water vapor absorption by **2** leads to a dramatic decrease of the exchange magnetic coupling between the copper(II) ions and thus to a drastic change of its powder EPR spectrum. These changes have been attributed to a chemical transformation involving the shifting of two carboxylates from bidentate bridging to monodentate non-bridging driven by the binding of water molecules to the copper ions. We have shown by IR spectroscopy that a reversible hydration/dehydration process is possible using vacuum/exposition to air cycles. Dehydration leads to a partial recovery of the antiferromagnetic coupling of the initial complex **2** as evidenced by the EPR and magnetic data. These data indicate that the structural transformation occurring upon the hydration/dehydration process is not reversible, the paddlewheel structure being not recovered. However, dehydration induces a structural change within the solid, most probably a change in the coordination mode of the carboxylates. Overall, these results show that fluorous compounds can experience very large and efficient structural reorganisation in the solid state driven by external stimuli/compounds. Such behavior has already been exploited by Metrangolo, Resnati and coworkers to develop non-porous crystalline materials which can, nonetheless, selectively and dynamically trap guest compounds [27]. Our further studies will attempt to develop a fully reversible process. This could be achieved by a better control of the hydration process and by tuning the fluorous–fluorous interactions within the crystal to favor a single-crystal-to-single-crystal transformation when hydrating **2**.

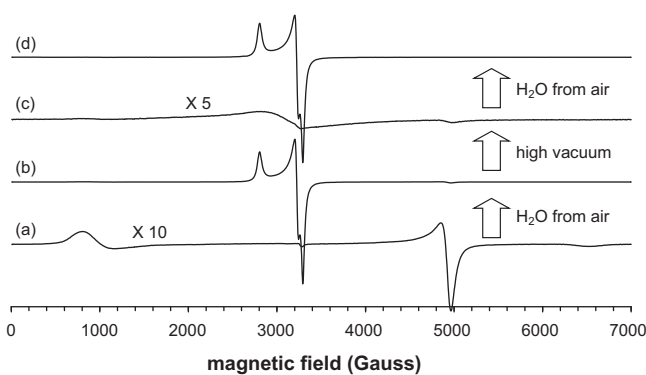


Fig. 5. Room temperature X-band powder EPR spectra of (a) **2**, (b) after exposure of **2** in air for 110 min corresponding to hydrated **2**, (c) after exposure of hydrated **2** to high vacuum (7×10^{-5} mbar) for 4 h and, (d) after re-exposure of the same sample to air for \sim 15 min.

4. Experimental

4.1. General

All reagents were obtained from commercial sources and used as received unless noted otherwise. The acetone and NEt_3 used for the synthesis of **4** were dried over K_2CO_3 and CaH_2 , respectively, and distilled prior to use. Air sensitive samples were prepared in an M. Braun (MB 150B-G) inert atmosphere glovebox under an N_2 atmosphere. Infrared spectra were recorded directly on crystals or powdered samples on a Perkin Elmer Spectrum 100 FTIR spectrometer at room temperature equipped with a Pike MiracleTM single reflection ATR system. The spectra (from 4000 to 650 cm^{-1}) were obtained from 20 scans, with a resolution of 1 cm^{-1} . Electronic absorption spectra were recorded on a Hitachi U3300 spectrophotometer (200–1000 nm scan range). The magnetic properties were carried out with a MPMS-5S Quantum Design SQuID (Superconducting Quantum Interference Device) magnetometer operating with an external magnetic field of 1 T within the range of 2–300 K. The measurements (data in blue, Fig. 6) were performed on a powdered sample of hydrated **2** which has been dehydrated under high vacuum and then transferred ($m = 20.8\text{ mg}$) in a glovebox and placed in a plastic bag which is sealed to avoid rehydration. The X-band EPR spectra were recorded with a Bruker EMX, equipped with the ER-4192 ST and ER-5106 QTW Bruker cavities, respectively.

4.2. Synthesis of $[\text{Cu}(\text{C}_8\text{F}_{17}\text{CO}_2)_4](\text{HNEt}_3)$ (2)

A dry acetone solution (2 mL) of a mixture of NEt_3 (0.357 g, 3.53 mmol) and $\text{C}_8\text{F}_{17}\text{CO}_2\text{H}$ (0.779 g, 1.68 mmol) is stirred for 30 min at room temperature whereupon the solvent and the excess of NEt_3 are evaporated under vacuum to afford $\text{C}_8\text{F}_{17}\text{CO}_2\text{HNEt}_3$ as a white solid (0.392 g, 98%). The solid is then dissolved in dry acetone (2 mL) to which a dry acetone (2 mL) solution of $\text{Cu}(\text{OTf})_2$ (0.128 g, 0.35 mmol) is added dropwise with stirring affording a blue solution. Large blue parallelepipedic X-ray quality crystals were grown by allowing the solution to stand at $-18\text{ }^\circ\text{C}$ for several days (68% yield). FTIR (crystal, major peaks): 3075, 3000, 1702, 1670 (sh), 1490, 1411, 1368, 1250, 1195, 1145, 971, 809, 730, 675; UV-vis (MeOH) [λ_{max} , nm (ε , $\text{M}^{-1}\text{ cm}^{-1}$)]: 790 (broad band, 40).

4.3. Crystallographic data collections and structural determinations

Crystallographic studies of complex **4** were performed at 150 K. A small crystal of approximate dimensions $0.15\text{ mm} \times 0.12\text{ mm} \times 0.05\text{ mm}$ was selected on a polarized microscope and mounted on a Bruker-Nonius κ -CCD diffractometer, Mo $\text{K}\alpha$ radiation (0.71073 \AA), φ scans, 1.6° per rotation frame, 93 s per frame, distance crystal-detector of 45 mm. The unit cell determination and data reduction were performed using the denzo and scalepack program [28] on the full set of data.

The structural determination was carried out by direct methods, and the refinement of atomic parameters based on full-matrix least-squares on F^2 was performed using the SHELX-97 programs [29] within the WINGX package [30] (CCDC 805012).

Acknowledgments

The CNRS (Salary Grant to A.M.), la Région Aquitaine (Salary Grant to A.M.) and the University of Bordeaux 1 are gratefully acknowledged for financial support.

References

- [1] (a) M. Melink, *Coord. Chem. Rev.* 36 (1981) 1–44;
(b) M. Melink, *Coord. Chem. Rev.* 42 (1982) 259–293;
(c) M. Kato, Y. Muto, *Coord. Chem. Rev.* 92 (1988) 45–88.
- [2] Y.R. Morgan, P. Turner, B.J. Kennedy, T.W. Hambley, P.A. Lay, J.R. Biffin, H.L. Regtop, B. Warwick, *Inorg. Chim. Acta* 324 (2001) 150–161.
- [3] F.P.W. Agterberg, H.A.J. Provo Kluit, W.L. Driessens, J. Reedijk, H. Oevering, W. Buijs, N. Veldman, M.T. Lakin, A.L. Speck, *Inorg. Chim. Acta* 267 (1998) 183–192.
- [4] M.R. Sundberg, R. Uggla, M. Melnik, *Polyhedron* 15 (1996) 1157–1163.
- [5] J.E. Weder, T.W. Hambley, B.J. Kennedy, P.A. Lay, G.J. Foran, A.M. Rich, *Inorg. Chem.* 40 (2001) 1295–1302.
- [6] R.D. Harcourt, F.L. Skrezenek, R.G.A.R. Maclagan, *J. Am. Chem. Soc.* 108 (1986) 5403–5408.
- [7] D. Maspoch, D. Ruiz-Molina, J. Veciana, *J. Mater. Chem.* 14 (2004) 2713–2723.
- [8] (a) S.V. Ley, A.W. Thomas, *Angew. Chem. Int. Ed.* 42 (2003) 5400–5449;
(b) S. Chiba, L. Zhang, J.-Y. Lee, *J. Am. Chem. Soc.* 132 (2010) 7266–7267.
- [9] (a) G. Psomas, C.P. Raptopoulou, L. Iordanidis, C. Dendrinou-Samara, V. Tangoulis, D. Kessissoglou, *Inorg. Chem.* 39 (2000) 3042–3048;
(b) J.C. Stephens, A.M. Khan, R.P. Houser, *Inorg. Chem.* 40 (2001) 5064–5065.
- [10] J.-M. Vincent, *J. Fluorine Chem.* 129 (2008) 903–909.
- [11] (a) M. El Bakkari, N. McClenaghan, J.-M. Vincent, *J. Am. Chem. Soc.* 124 (2002) 12942–12943;
(b) M. El Bakkari, B. Fronton, R. Luguya, J.-M. Vincent, *J. Fluorine Chem.* 127 (2006) 558–564.
- [12] M. Contel, P.R. Villuendas, J. Fernández-Gallardo, P.J. Alonso, J.-M. Vincent, R.H. Fish, *Inorg. Chem.* 44 (2005) 9771–9778.
- [13] M. El Bakkari, J.-M. Vincent, *Org. Lett.* 6 (2004) 2765–2767.
- [14] M. El Bakkari, R. Luguya, R. Correa da Costa, J.-M. Vincent, *New J. Chem.* 32 (2008) 193–196.
- [15] A. Motreff, G. Raffy, A. Del Guerro, C. Belin, M. Dussauze, V. Rodriguez, J.-M. Vincent, *Chem. Commun.* 46 (2010) 2617–2619.
- [16] A. Motreff, C. Belin, R. Correa da Costa, M. El Bakkari, J.-M. Vincent, *Chem. Commun.* 46 (2010) 6261–6263.
- [17] A. Motreff, R. Correa da Costa, H. Allouchi, M. Duttine, C. Mathonière, C. Duboc, J.-M. Vincent, *Inorg. Chem.* 48 (2009) 5623–5625.
- [18] (a) K. Nakatani, J.-Y. Carriat, Y. Journaux, O. Kahn, F. Lloret, J.P. Renard, Y. Pei, J. Sletten, M. Verdaguier, *J. Am. Chem. Soc.* 111 (1989) 5739–5748;
(b) J. Larionova, S.A. Chavan, J.V. Yakhmi, A. Gulbrandsen Frystein, J. Sletten, C. Sourisseau, O. Kahn, *Inorg. Chem.* 36 (1997) 6374–6381;
(c) N. Yanai, W. Kaneko, K. Yoneda, M. Ohba, S. Kitagawa, *J. Am. Chem. Soc.* 129 (2007) 3496–3497;
(d) D. Maspoch, D. Ruiz-Molina, K. Wurst, N. Domingo, M. Cavallini, F. Biscarini, J. Tejada, C. Rovira, J. Veciana, *Nat. Mater.* 2 (2003) 190–195;
(e) N. Guillou, C. Livage, W. van Beek, M. Noguès, G. Férey, *Angew. Chem. Int. Ed.* 42 (2003) 644–647;
(f) S.-I. Ohkoshi, K.I. Arai, Y. Sato, K. Hashimoto, *Nat. Mater.* 3 (2004) 857–861;
(g) X.-N. Cheng, W.-X. Zhang, Y.-Y. Lin, Y.-Z. Zheng, X.-M. Chen, *Adv. Mater.* 19 (2007) 1494–1498;
(h) X.-N. Cheng, W.X. Zhang, X.-M. Chen, *J. Am. Chem. Soc.* 129 (2007) 15738–15739;
(i) M. Kurmoo, H. Kumagai, K.W. Chapman, C.J. Kepert, *Chem. Commun.* (2005) 3012–3014;
(j) S.K. Ghosh, W. Kaneko, D. Kiriya, M. Ohba, S. Kitagawa, *Angew. Chem. Int. Ed.* 47 (2008) 8843–8847;
(k) Z. Wang, B. Zhang, H. Fujiwara, H. Kobayashi, M. Kurmoo, *Chem. Commun.* (2004) 416–417;
(l) Y. Sato, S.-I. Ohkoshi, K.-I. Arai, M. Tozawa, K. Hashimoto, *J. Am. Chem. Soc.* 125 (2003) 14590–15595;
(m) V. Niel, A.L. Thompson, M.C. Muñoz, A. Galet, A.E. Goeta, J.A. Real, *Angew. Chem. Int. Ed.* 42 (2003) 3760–3763.
- [19] O. Kahn, J. Larionova, J.Y. Vakhmi, *Chem. Eur. J.* 5 (1999) 3443–3449.
- [20] E.V. Karpova, A.I. Boltalin, M.A. Zakharov, N.I. Sorokina, Y.M. Korenev, S.I. Troyanov, Z. Anorg. Allg. Chem. 624 (1998) 741–744.
- [21] P. de Meester, S.R. Fletcher, A.C. Skapski, *J. Chem. Soc. Dalton Trans.* 23 (1973) 2575–2578.
- [22] K. Smolander, *Inorg. Chim. Acta* 114 (1986) 1–8.
- [23] A.C. Warden, M.T.W. Hearn, L. Spiccia, *Inorg. Chem.* 42 (2003) 7037–7040.
- [24] S.W. Ng, X.-M. Chen, G. Yang, *Acta Crystallogr. C* 54 (1998) 1389–1393.
- [25] G. Psomas, C.P. Raptopoulou, L. Iordanidis, C. Dendrinou-Samara, V. Tangoulis, D.P. Kessissoglou, *Inorg. Chem.* 39 (2000) 3042–3048.
- [26] F.A. Cotton, E.V. Dikarev, M.A. Petrukhina, *Inorg. Chem.* 39 (2000) 6072–6079.
- [27] P. Metrangolo, Y. Carcenac, M. Lahtinen, T. Pilati, K. Rissanen, A. Vij, G. Resnati, *Science* 323 (2009) 1461–1464.
- [28] COLLECT, Nonius, Delft, The Netherlands, 1998.
- [29] G.M. Sheldrick, *Programs for Crystal Structure Analysis*, University of Göttingen, Göttingen, Germany, 1998.
- [30] L.J. Farrugia, *J. Appl. Crystallogr.* 32 (1999) 837–838.